Nonlinear Dyn (2020) 100:1275–1287
https://doi.org/10.1007/s11071-020-05574-x

ORIGINAL PAPER

Fuzzy neural network-based chaos synchronization for a class of fractional-order chaotic systems: an adaptive sliding mode control approach

RenMing Wang · YunNing Zhang · YangQuan Chen · Xi Chen · Lei Xi

Received: 22 June 2019 / Accepted: 11 March 2020 / Published online: 21 March 2020

Abstract This paper deals with chaos synchronization problem between two different uncertain fractional-order (FO) chaotic systems with disturbance based on FO Lyapunov stability analysis method. A T–S fuzzy neural network model as a universal approximator is constructed to approximate those uncertain terms and unknown parameters. An adaptive sliding mode control scheme is established, and the adaptive sliding mode control design procedure is proposed, which not only guarantees the stability and robustness of the proposed control method, but also guarantees that the external disturbance on the synchronization error can be attenuated. Finally, simulation results show applicability and feasibility of the proposed control strategy.

Keywords Fractional-order system · Fuzzy neural network · Chaos synchronization · Sliding mode control

1 Introduction

In recent years, fractional-order systems (FOSs) have been receiving intensive studies because the underlying facts about the fractional differentiation are significantly different from those of the integer-order counterparts. Also, numerous physical systems are described more accurately by FO differential equations, for instance dielectric polarization, electromagnetic waves and viscoelastic systems [1], heat and fluid flow processes [2], flight control in uncrewed aerial vehicles [3], and so on. Thus, several results related to stability analysis and control design of FO systems have been reported [4–8]. Many FO control methods including FO sliding mode control [5], FO neural network control [9], FO adaptive control [10,11], and so on, have been derived by integrating some classic control approaches and FO operators. Despite so, researchers are still interested in the FO systems and FO control design due to many interesting dynamical behaviors such as existence of limit cycle and chaotic behaviors have been observed in FO nonlinear systems [12,13], which leads the researchers obviously to the investigation of chaotic characteristic, chaos suppression and synchronization of such systems [14,15]. It should be pointed out that the control techniques for integer-order systems may not to be extended directly to the FO cases. As a result, the chaotic characteristic analysis and chaos synchronization for FO systems is still an attractive and challenging problem, which motivates the work.

A lots of efforts have been devoted to the study of chaotic synchronization control for FO chaotic systems over past few decades due to its potential applications in secure communication and control process-

R. Wang (✉) · Y. Zhang · X. Chen · L. Xi
College of Electrical Engineering and Renewable Energy, China Three Gorges University, Yichang 443002, People's Republic of China
e-mail: eermwang@ctgu.edu.cn

Y. Chen
University of California, Merced, CA 95343, USA
e-mail: ychen53@ucmerced.edu

ing [16–23]. To mention a few, in [16], for instance, two FO hyperchaotic systems can be synchronized based on Lyapunov stability theorem by using direct adaptive interval type 2 fuzzy active sliding control approach. In [20], the impulsive synchronization of fractional-order discrete-time chaotic systems is discussed. In addition, the adaptive synchronization problem of fractional-order memristor-based neural networks with time delay is investigated in [24] by combining the adaptive control, linear delay feedback control, with a fractional-order inequality. The problem of synchronization of FO complex-valued neural networks with time delays is discussed in [25]. The investigation of FO chaos synchronization meets technical obstacles due to the fact that the actual systems have uncertain parameters or uncertain system structure, or it is difficult to be described accurately. One of the most efficient solutions to such problem is probably adaptive control scheme based on fuzzy neural network, which is extensively used for approximating uncertain terms or unknown parameters, which is just as done in [16–18,23,26]. It should be noted that the considered system structure in [16] is known and fuzzy network is used only to approximate the upper bound of disturbance. However, it is difficult to design a controller with the above-mentioned technique when neither the system structure nor the upper bound of disturbance is known. A typical issue we have to face is the issue of approximating the unknown parameters of the considered system. Therefore, how to overcome this obstacle to design a controller for chaos synchronization of FO systems is a open problem, which is another motivation of this work.

To the best of our knowledge, chaos synchronization problem between two different uncertain FO chaotic systems with disturbance has still not been fully investigated in the existing studies. Inspired by the results in [17], chaos synchronization problem between two different uncertain FO chaotic systems based on adaptive fuzzy sliding mode control technique is investigated in this paper. The main contributions of this work are listed as follows.

(1) A adaptive sliding mode control technique is established for chaos synchronization of uncertain FO chaotic systems.
(2) A T–S fuzzy neural network model as a universal approximator is constructed to approximate the unknown functions and disturbances, and FO adaptive laws are designed to update the neuro-fuzzy parameters.

This paper is organized as follows: In Sect. 2, an introduction to fractional derivative and its relation to the approximation solution and some lemmas are addressed. Problem formulation and a brief introduction of the fuzzy neural networks are presented in Sect. 3, and in this section, a controller is designed by sliding mode method with fuzzy neural network model used as an approximator. In Sect. 4, the synchronization error and system stability are analyzed by a FO Lyapunov approach. In Sect. 5, application of the proposed method on FO expression of chaotic system is investigated and the results of numerical simulation are shown. The conclusion is given in Sect. 6.

2 Basic definition and preliminaries for fractional-order systems

Fractional calculus can describe and model real objects more accurately than classical "integer-order" methods. Fractional calculus is denoted by ${}_aD_t^q$, which is a notation for taking both the fractional integral and derivative in an expression defined as

$$ {}_aD_t^q = \begin{cases} \frac{\mathrm{d}^q}{\mathrm{d}t^q}, & q > 0 \\ 1, & q = 0 \\ \int_a^t (\mathrm{d}\tau)^q, & q < 0. \end{cases} \tag{1} $$

There are three most common definitions of fractional differential integral in the literature. One of them is Caputo's derivative, which is used in this paper, defined as:

$$ {}_aD_t^q f(t) = \frac{1}{\Gamma(m-q)} \int_a^t \frac{f^m(\tau)}{(t-\tau)^{1-(m-q)}} \mathrm{d}\tau, \tag{2} $$

where $m-1 < q < m$ and Γ is the Gamma function.

The numerical simulation of a fractional differential equation is not simple as that of an ordinary differential equation. In our case, the fractional Adams–Bashforth–Moulton method is chosen as a representative numerical scheme [27]. To explain this method, the following differential equation is considered

$$ \begin{cases} D_t^q y(t) = r(t, y(t)), & 0 \le t \le T, \\ y^{(k)}(0) = y_0^{(k)}, & k = 0, 1, \ldots, m-1. \end{cases} \tag{3} $$

The solution of Eq. (3) is equivalent to Eq. (4)

$$y(t) = \sum_{k=0}^{\lceil q\rceil-1} y_0^{(k)} \frac{t^k}{k!} + \frac{1}{\Gamma(q)} \int_0^t (t-s)^{q-1} r(s, y(s))\, \mathrm{d}s. \tag{4}$$

Setting $h = T/N$, $t_n = nh$, $n = 0, 1, \ldots, N$, Eq. (4) can be discretized as follows:

$$y_h(t_{n+1}) = \sum_{k=0}^{\lceil q\rceil-1} y_0^{(k)} \frac{t^k}{k!} + \frac{h^q}{\Gamma(q+2)} r\left(t_{n+1}, y_h^p(t_{n+1})\right) + \frac{h^q}{\Gamma(q+2)} \sum_{j=0}^{n} a_{j,n+1} r(t_j, y_h(t_j)), \tag{5}$$

where

$$y_h^p(t_{n+1}) = \sum_{k=0}^{\lceil q\rceil-1} y_0^{(k)} \frac{t^k}{k!} + \frac{1}{\Gamma(q)} \sum_{j=0}^{n} b_{j,n+1} r(t_j, y_h(t_j)),$$

$$a_{j,n+1} = \begin{cases} n^{q+1} - (n-q)(n+1)^q, & j = 0 \\ (n-j+2)^{q+1} + (n-j)^{q+1} & \\ \quad -2(n-j+1)^{q+1}, & 1 \le j \le n \\ 1, & j = n+1 \end{cases} \tag{6}$$

and

$$b_{j,n+1} = \frac{h^q}{q}((n+1-j)^q - (n-j)^q).$$

The approximation error is described as

$$\max_{j=0,1,\ldots,N} \left|y(t_j) - y_h(t_j)\right| = 0(h^p),$$

where $p = \min(2, 1+q)$.

In the rest of this paper, the operator D^q denotes the Caputo's fractional differential operator of order q. The following lemmas will be used later.

Lemma 1 [28] *For the FO system* (7)

$$D^q x(t) = f(x(t)), \tag{7}$$

with $q \in (0, 1)$, $x \in \mathbb{R}^n$ is the state vector and $x = \boldsymbol{0}$ is the equilibrium point of (7)*, the equilibrium point of system* (7) *is stable if*

$$x(t) f(x(t)) \le 0, \quad \forall x \ne 0.$$

And the equilibrium point is asymptotically stable if

$$x(t) f(x(t)) < 0, \quad \forall x \ne 0.$$

Lemma 2 [28] *Let $x(t) \in \mathbb{R}^n$ be continuous and differentiable. Then, the following inequality holds for any time instant $t \ge t_0$*

$$\frac{1}{2} D^q x^2(t) \le x(t) D^q x(t), \quad \forall q \in (0, 1).$$

Lemma 3 [29] *For a given linear autonomous FO system*

$$D^q x(t) = Ax(t), \tag{8}$$

the zero solution to system (8) *is asymptotically stable if all eigenvalues λ_i, $(i = 1, 2, \ldots, n)$ of matrix A satisfy*

$$|\arg(\lambda_i)| > q\frac{\pi}{2},$$

where $0 < q \le 1$.

Lemma 4 [30] *The trivial solution of system* (7) *is asymptotically stable if there exists a positive definite Lyapunov function $V(x(t))$ such that $D^q V(x(t)) < 0$ for all $t > 0$.*

3 Problem formulation and controller design

Consider the synchronization of the following two N-dimension FO chaotic systems, the master system:

$$\begin{cases} D^q x_i = x_{i+1}, & 1 \le i \le n-1 \\ D^q x_n = g(x, t), \end{cases} \tag{9}$$

and the slave system:

$$\begin{cases} D^q y_i = y_{i+1}, & 1 \le i \le n-1 \\ D^q y_n = f(y, t) + d(t) + u(t), \end{cases} \tag{10}$$

where $x_i, y_i \in R$, $(i = 1, 2, \ldots, n)$ are system states, $x = [x_1, x_2, \ldots, x_n]^{\mathrm{T}}$, $y = [y_1, y_2, \ldots, y_n]^{\mathrm{T}}$, $f(y, t)$ and $g(x, t)$ are unknown but bounded functions, $d(t)$ is unknown bounded disturbance, $u(t)$ is the controller to be designed.

Define the synchronization error as

$$e_i = y_i - x_i, \quad (i = 1, 2, \ldots, n); \tag{11}$$

then, the following error dynamic is obtained

$$\begin{cases} D^q e_1 = e_2, \\ D^q e_2 = e_3, \\ \vdots \\ D^q e_n = f(y, t) - g(x, t) + d(t) + u(t), \end{cases} \tag{12}$$

where $\mathbf{e} = [e_1, e_2, \ldots, e_n]^{\mathrm{T}}$ is the error vector.

Consider the following sliding mode function

$$s = -\mathbf{ce} = -(c_1 e_1 + c_2 e_2 + \cdots + c_{n-1} e_{n-1} + e_n), \tag{13}$$

where $\mathbf{c} = [c_1, c_2, \ldots, c_{n-1}, 1]$ is a constant vector to be designed satisfying condition in Lemma 3 so that the sliding mode surface vanishes quickly. The process can be classified into two phases: One is the approaching phase with $s \neq 0$ and the other is the sliding phase with $s = 0$. Our objective is to design the control effort such that the sliding mode condition $s D^q s \leq -\eta_\Delta |s|$ (η_Δ is a given positive constant) is satisfied which, by Lemma 1, can guarantee that the trajectory of the synchronization error vector $\mathbf{e}$ moves from approaching phase to sliding phase.

In view of (12) and (13), the following equation holds

$$\begin{aligned} D^q s &= -\mathbf{c} D^q \mathbf{e} \\ &= -[c_1 e_2 + c_2 e_3 + \ldots + c_{n-1} e_n + f(y,t) \\ &\quad - g(x,t) + d(t) + u(t)]. \end{aligned} \tag{14}$$

Consequently, the control effort can be designed, by the idea of equivalent control, as

$$\begin{cases} u = u_{eq} + u_d, \\ u_{eq} = -\sum_{i=1}^{n-1} c_i e_{i+1} - f(y,t) + g(x,t), \\ u_d = \eta \text{sign}(s), \end{cases} \tag{15}$$

where $\eta \geq \eta_\Delta > 0$, $f(y,t)$, $g(x,t)$ and η are all unknown. These unknown functions and parameter make the control effort (15) not implementable. In order to identify these variables and parameters, a T–S fuzzy neural network model which includes a fuzzy logic system and a neural network is introduced as shown in Fig. 1.

Fuzzy logic systems address the imprecision of input and output variables directly by defining them with fuzzy numbers (and fuzzy sets) that can be expressed in linguistic terms. The basic configuration of the T–S fuzzy neural network (FNN) system includes a fuzzy rule base, which consists of a collection of fuzzy if–then rules in the following form:

$$R^{(i)} : if\ x_i\ is\ A_1^i \text{ and } \ldots \text{ and } x_n \text{ is } A_n^i \text{ then } y \text{ is } B^i,$$

where $A_1^i, A_2^i, \ldots A_n^i$ and B^i are fuzzy sets. The output of the fuzzy logic system with central average defuzzifier, product inference and singleton fuzzifier can be expressed as

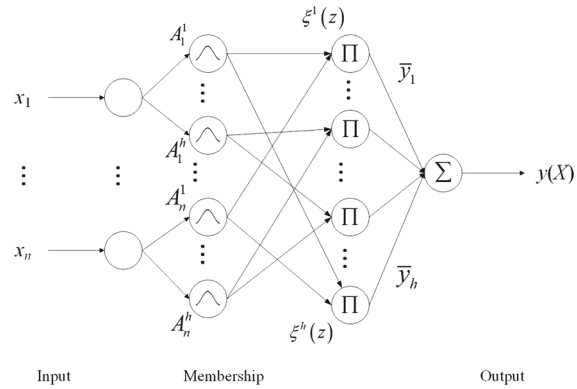

Fig. 1 Configuration of the T–S fuzzy neural networks

$$y(X) = \frac{\sum_{i=1}^{h} \bar{y}^i \left(\prod_{j=1}^{n} \mu_{A_j^i(x_j)} \right)}{\sum_{i=1}^{h} \left(\prod_{j=1}^{n} \mu_{A_j^i(x_j)} \right)} = \theta^T \xi(X), \tag{16}$$

where h is the number of fuzzy rules, $\mu_{A_j^i(x_j)}$ is the membership function value of the fuzzy variable which is commonly selected as Gaussian function and $\theta^T = [\bar{y}_1^T, \bar{y}_2^T, \ldots, \bar{y}_h^T]$ is an adjustable parameter vector. Fuzzy basis function vector is defined as

$$\xi^i(X) = \frac{\prod_{j=1}^{n} \mu_{A_j^i(x_j)}}{\sum_{i=1}^{h} \left(\prod_{j=1}^{n} \mu_{A_j^i(x_j)} \right)}. \tag{17}$$

The layer 1 and layer 2 of this network are used for input and membership function, respectively, and layer 3 is used for product fuzzy basis function vector. Network output with adjustable parameter vector can be obtained in layer 4, namely

$$y(X) = \theta^T \xi(X). \tag{18}$$

The above fuzzy logic system can uniformly approximate any well-defined nonlinear function over a compact set to any degree of accuracy by the universal approximation theorem [31]. Also it is straightforward to show that a multi-output system can always be approximated by a group of single-output approximation systems.

Hence, the approximation values of $f(y,t)$, $g(x,t)$ and η via the T–S fuzzy neural network can be expressed as:

$$\hat{f}\left(y, \theta_y\right) = \hat{\theta}_y^T \xi_y\left(y\right),$$
$$\hat{g}\left(x, \theta_x\right) = \hat{\theta}_x^T \xi_x\left(x\right),$$

$$\hat{\eta}\left(e,\theta_e\right)=\hat{\theta}_e^T\xi_e\left(e\right). \tag{19}$$

Substituting (19) into (15), the control effort can be rewritten as

$$u=-\sum_{i=1}^{n-1}c_ie_{i+1}-\hat{f}\left(y,t\right)+\hat{g}\left(x,t\right)+\hat{\eta}\text{sign}\left(s\right). \tag{20}$$

Define optimal parameter estimations of $f(y,t)$, $g(x,t)$ and η as

$$\begin{aligned}\theta_f^*&=\underset{\theta_f\in\Omega_f}{\arg\min}\left[\sup_{y\in\Omega_y}|\hat{f}(y\mid\theta_f)-f(y,t)|\right],\\ \theta_g^*&=\underset{\theta_g\in\Omega_g}{\arg\min}\left[\sup_{x\in\Omega_x}|\hat{g}(x\mid\theta_g)-g(x,t)|\right],\\ \theta_\eta^*&=\underset{\theta_e\in\Omega_\eta}{\arg\min}\left[\sup_{e\in\Omega_e}|\hat{\eta}(e\mid\theta_\eta)-\eta|\right],\end{aligned} \tag{21}$$

and some constraint sets of suitable bounds as

$$\begin{aligned}&\Omega_f=\{f\mid|f|\le M_f\},\quad \Omega_g=\{g\mid|g|\le M_g\},\\ &\Omega_\eta=\{\eta\mid\eta\le M_\eta\},\quad \Omega_y=\{y\mid|y|\le M_y\},\\ &\Omega_x=\{x\mid|x|\le M_x\},\quad \Omega_e=\{e\mid|e|\le M_e\},\end{aligned} \tag{22}$$

separately, where M_f, M_g, M_η, M_y, M_x, M_e are uncertain positive constants. The block diagram of the controlled system is illustrated in Fig. 2.

4 Synchronization error and system stability analysis

Consider the Lyapunov function candidate

$$V=\frac{1}{2}s^2+\frac{1}{2r_f}\tilde{\theta}_f^T\tilde{\theta}_f+\frac{1}{2r_g}\tilde{\theta}_g^T\tilde{\theta}_g+\frac{1}{2r_\eta}\tilde{\theta}_\eta^T\tilde{\theta}_\eta, \tag{23}$$

where r_f, r_g and r_η are positive constants and $\tilde{\theta}_f$, $\tilde{\theta}_g$, and $\tilde{\theta}_\eta$ are defined as

$$\begin{aligned}\tilde{\theta}_f&=\hat{\theta}_f-\theta_f^*,\\ \tilde{\theta}_g&=\hat{\theta}_g-\theta_g^*,\\ \tilde{\theta}_\eta&=\hat{\theta}_\eta-\theta_\eta^*.\end{aligned} \tag{24}$$

Taking the q-order derivative of (23) with respect to time and utilizing Lemma 2 and (24), we get

$$\begin{aligned}D^qV&\le sD^qs+\frac{1}{r_f}\tilde{\theta}_f^TD^q\tilde{\theta}_f\\ &\quad+\frac{1}{r_g}\tilde{\theta}_g^TD^q\tilde{\theta}_g+\frac{1}{r_\eta}\tilde{\theta}_\eta^TD^q\tilde{\theta}_\eta\\ &\le sD^qs+\frac{1}{r_f}\tilde{\theta}_f^TD^q(\hat{\theta}_f-\theta_f^*)\\ &\quad+\frac{1}{r_g}\tilde{\theta}_g^TD^q(\hat{\theta}_g-\theta_g^*)\\ &\quad+\frac{1}{r_\eta}\tilde{\theta}_\eta^TD^q(\hat{\theta}_\eta-\theta_\eta^*)\\ &\le sD^qs+\frac{1}{r_f}\tilde{\theta}_f^TD^q\hat{\theta}_f+\frac{1}{r_g}\tilde{\theta}_g^TD^q\hat{\theta}_g\\ &\quad+\frac{1}{r_\eta}\tilde{\theta}_\eta^TD^q\hat{\theta}_\eta.\end{aligned} \tag{25}$$

In view of (13), (15) and (20), (14) can be further expressed as

$$\begin{aligned}D^qs=&-\left(f(y,t)-f^*(y,t)+f^*(y,t)-\hat{f}(y,t)\right)\\ &+g(x,t)-g^*(x,t)+g^*(x,t)\\ &-\hat{g}(x,t)-d(t)-\hat{\eta}\text{sign}(s),\end{aligned} \tag{26}$$

where

$$\begin{aligned}f^*\left(y,\theta_f\right)&=\theta^{*T}_y\xi_y\left(y\right),\\ g^*\left(x,\theta_g\right)&=\theta^{*T}_x\xi_x\left(x\right),\\ \eta^*\left(e,\theta_\eta\right)&=\theta^{*T}_\eta\xi_e\left(e\right),\end{aligned} \tag{27}$$

are optimal estimations of functions f, g and η.

Define the optimal approximation error as

$$\begin{aligned}d_d\left(t\right)=&-\left(f\left(y,t\right)-f^*\left(y,t\right)\right)\\ &+\left(g\left(x,t\right)-g^*\left(x,t\right)\right).\end{aligned}$$

With (19) and (27), (26) is rewritten as

$$\begin{aligned}D^qs=&-\left(\theta^{*T}_y-\hat{\theta}_y^T\right)\xi_y\left(y\right)+\left(\theta^{*T}_x-\hat{\theta}_x^T\right)\xi_x\left(x\right)\\ &+d_d\left(t\right)-d\left(t\right)-\left(\hat{\theta}_e^T\xi_e\left(e\right)\right)\text{sign}(s).\end{aligned} \tag{28}$$

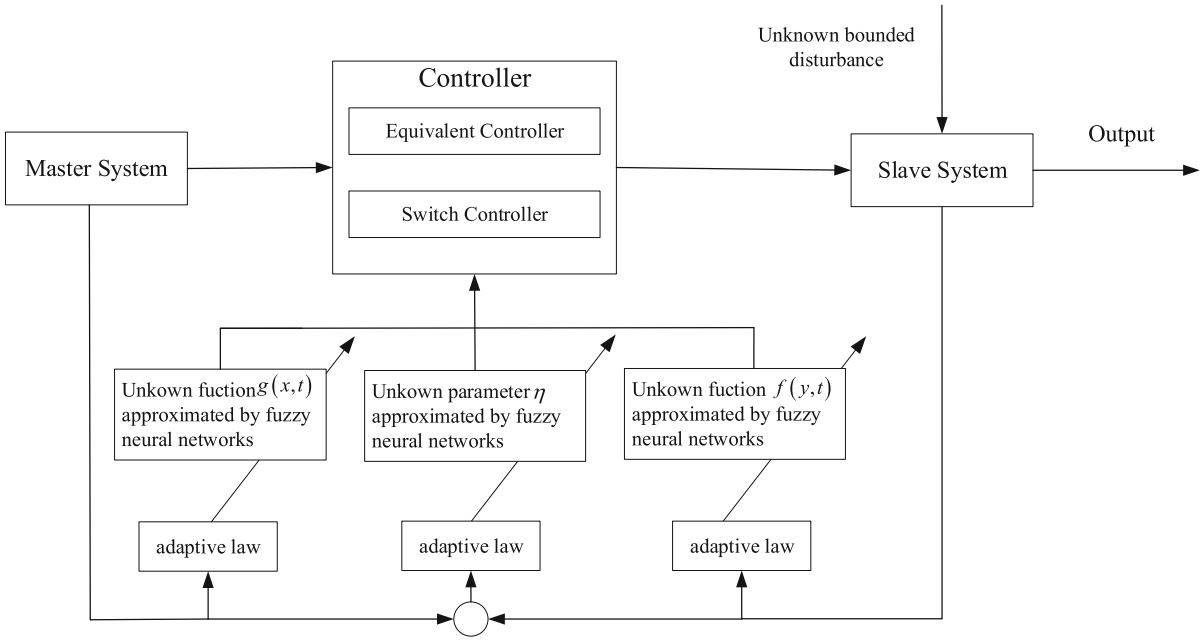

Fig. 2 Block diagram of the controlled system

Substituting (28) into (25), the following inequality holds

$$\begin{aligned} D^q V \leq\ & s\left(\tilde{\theta}_f^T \xi_y(y) - \tilde{\theta}_g^T \xi_x(x) + d_d(t) - d(t)\right) \\ & - s\left(\tilde{\theta}_\eta^T \xi_e(e)\, signs + \theta^{*T}_\eta \xi_e(e)\, signs\right) \\ & + \frac{1}{r_f}\tilde{\theta}_f^T D^q \hat{\theta}_f + \frac{1}{r_g}\tilde{\theta}_g^T D^q \hat{\theta}_g + \frac{1}{r_\eta}\tilde{\theta}_\eta^T D^q \hat{\theta}_\eta \\ \leq\ & \tilde{\theta}_f^T \left(\frac{1}{r_f} D^q \hat{\theta}_f + s\xi_y(y)\right) \\ & + \tilde{\theta}_g^T \left(\frac{1}{r_g} D^q \hat{\theta}_g - s\xi_x(x)\right) \\ & + \tilde{\theta}_\eta^T \left(\frac{1}{r_\eta} D^q \hat{\theta}_\eta - |s|\,\xi_e(e)\right) \\ & + s\left(d_d(t) - d(t)\right) - \left(\theta^{*T}_\eta \xi_e(e)\right)|s|. \end{aligned} \tag{29}$$

Now, defining the adaptive laws of adjustable parameter vectors as

$$\begin{aligned} D^q \hat{\theta}_f &= -r_f s \xi_y(y), \\ D^q \hat{\theta}_g &= r_g s \xi_x(x), \\ D^q \hat{\theta}_\eta &= r_\eta |s|\, \xi_e(e), \end{aligned} \tag{30}$$

and substituting (30) into (29), we have

$$\begin{aligned} D^q V &= s\left(d_d(t) - d(t)\right) - |s|\,\theta^{*T}_\eta \xi_e(e) \\ &= |s|\,|d_d(t) - d(t)| - |s|\,\eta^*. \end{aligned} \tag{31}$$

It is the fact, by the assumptions in (22) that d_d is bounded which together with the assumption that disturbance $d(t)$ is bounded, one can obtain the following inequalities with some positive constant η^*

$$\begin{aligned} & |d_d(t) - d(t)| - \eta^* < 0, \\ & D^q V \leq |s|\left(|d_d(t) - d(t)| - \eta^*\right) < 0. \end{aligned} \tag{32}$$

Therefore, $D^q V < 0$ holds, which means that, by Lemma 4, asymptotical stability of system (12) is guaranteed and synchronization of systems (9) and (10) can be achieved with controller (20) and the adaptive law (30). Hence, the following result is obtained.

Theorem 1 *Consider two N-dimension FO chaotic systems, master system* (9) *and slave system* (10)*, and the control effort of the slave system is given in* (15) *with the fuzzy adaptive laws in* (30)*. Then, under the effect of controller* (20)*, the resulting closed-loop system is global asymptotically stable and the synchronization error will converge to zero asymptotically.*

Remark 1 It is worth noting that the undesired chattering phenomenon is unavoidable when the sign function is introduced to controller design in (15) to estimate the effect caused by external disturbances and approximation errors. To solve the problem, the sigmoid function with good smoothness is used to replace the sign func-

tion, so that it can not only realize the function of sign function but also restrain the chattering phenomenon.

5 Simulation examples

In this section, we will consider two examples to illustrate the effectiveness of our proposed design method.

Example 1 Consider the chaos synchronization of two nonidentical FO uncertain chaotic systems with the order $q = 0.98$, which is chosen from [32].

Master system: FO Duffing–Holmes system

$$\begin{cases} D^q x_1 = x_2, \\ D^q x_2 = x_1 - a x_2 - x_1^3 + b\cos(t) + d_x(t). \end{cases} \tag{33}$$

Slave system: FO Gyros system

$$\begin{cases} D^q y_1 = y_2, \\ D^q y_2 = -\epsilon^2 \frac{(1-\cos y_1)^2}{(\sin y_1)^3} \\ -\beta \sin y_1 - \psi_1 y_1 - \psi_2 y_2^3 \\ \quad +(\beta + \lambda \sin(\omega t)) \sin y_1 + u + d_y(t). \end{cases} \tag{34}$$

The parameters are chosen as

$$\begin{aligned} &a = 0.25, \quad b = 0.3, \ \epsilon = 10, \ \beta = 1, \ \psi_1 = 0.5, \\ &\psi_2 = 0.05, \ \omega = 2, \quad \lambda = 35, \ r_f = r_g = r_\eta = 50. \end{aligned} \tag{35}$$

Under the selected parameters, the equilibrium of system (33) is unstable, which can be verified by using the first Lyapunov method. In fact, there are two real eigenvalues of the Jacobian matrix, one of which is positive, in the equilibrium point of system (33). Also, the maximum Lyapunov exponent of system (33) is computed as 0.0773, which shows the FO Duffing–Holmes system is chaotic. The Lyapunov exponent spectrums are shown in Fig. 3.

For the purpose of numerical simulations, it is assumed that the external disturbances are $d_x(t) = 0.1\cos(3t)$ in the master system and $d_y(t) = 0.2\cos(t)$ in the slave system, respectively. The initial values of the master and slave systems are set as $x(0) = [0.3, -0.2]^{\mathrm{T}}$ and $y(0) = [-0.1, 0.2]^{\mathrm{T}}$, respectively.

The phase portrait of the FO Duffing–Holmes master system and FO Gyros slave system without control effort is depicted in Fig. 4, which shows the dynamic behaviors of the two systems are different. The membership functions for x_i and y_i, $(i = 1, 2)$ are selected as the following Gaussian functions:

$$\mu A_1^i(x_i) = \exp[-(x_i + 4)^2],$$

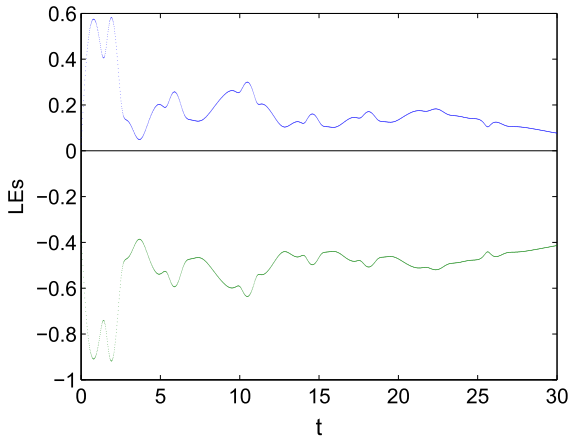

Fig. 3 Lyapunov exponent spectrums of system (33)

$$\begin{aligned} \mu A_2^i(x_i) &= \exp[-(x_i + 2)^2], \\ \mu A_3^i(x_i) &= \exp[-(x_i)^2], \\ \mu A_4^i(x_i) &= \exp[-(x_i - 2)^2], \\ \mu A_5^i(x_i) &= \exp[-(x_i - 4)^2]. \end{aligned} \tag{36}$$

Refer to remark 1. By computing the adaptive laws in (30) and the estimated values of variables and parameters in (19), with sliding mode surface $s = -150e_1 - e_2$, the control effort of the slave system can be obtained as

$$u(t) = -c_1 e_2 - \hat{f}(y, t) + \hat{g}(x, t) + \hat{\eta}\mathrm{simoid}(-3s). \tag{37}$$

Under the control effort of (37), the phase portrait of the synchronization performance of the master and slave systems is shown in Fig. 5. Figures 6 and 7 show the synchronization error dynamics e_1 and e_2, respectively. Figures 8 and 9 show the trajectories of the states x_1, y_1 and x_2, y_2, respectively. It is noticeable that the tracking error (or synchronization error) converges to zero asymptotically. The dynamic behavior of sliding mode surface $s(t)$ is shown in Fig. 10. Obviously, the value of switching surface converges to zero speedily. It is also noticeable that the chattering phenomenon, which is usually considered as a drawback of conventional sliding mode control, does not appear in our design.

For the sake of comparison, systems (33) and (34) are also simulated by using the method proposed in [32] with the same uncertainties and external disturbances. The simulation results are shown in Fig. 11. To compare with our method, the better synchronization result can be obtained from the perspective of the synchronization

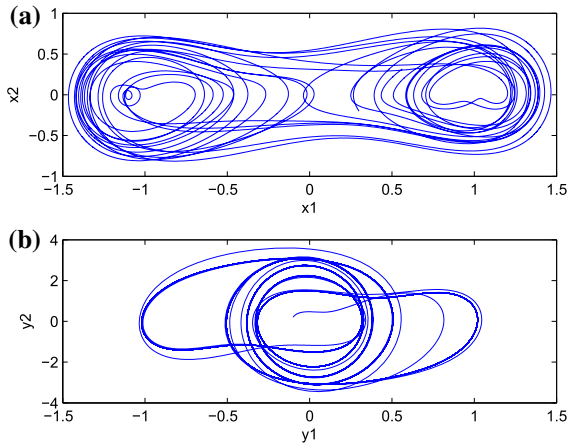

Fig. 4 Phase portrait of master and slave systems without control. **a** FO Duffing–Holmes system and **b** FO Gyros system

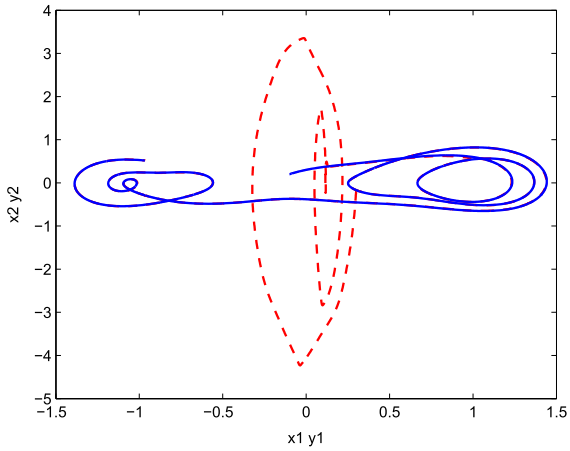

Fig. 5 Phase portrait of Duffing–Holmes master system and Gyros slave system with control

time of states by utilizing our method, which further highlights the validity and superiority of our control method.

Example 2 Let us consider two different uncertain fractional-order Jerk chaotic systems with the order $q = 0.95$ as follows.

Master system:

$$\begin{cases} D^q x_1 = x_2, \\ D^q x_2 = x_3, \\ D^q x_3 = a_{21} x_3 - x_2 + x_1 + b_{21} \sinh(x_1) \end{cases} \tag{38}$$

Slave system:

$$\begin{cases} D^q y_1 = y_2, \\ D^q y_2 = y_3, \\ D^q y_3 = a_{22} y_3 - y_2 + y_1 \\ \quad + b_{22} \sinh(y_1) + u(t) + d(t) \end{cases} \tag{39}$$

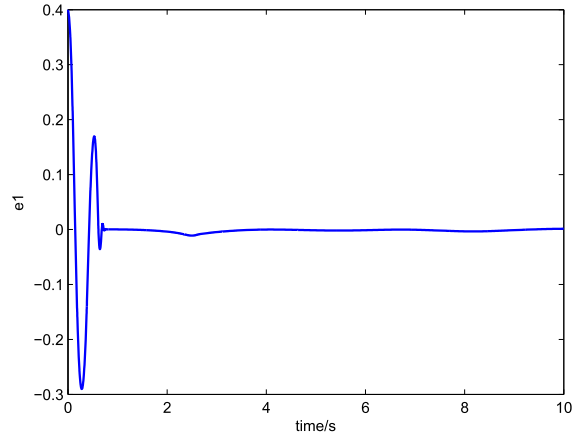

Fig. 6 Error dynamics of the states x_1 and y_1

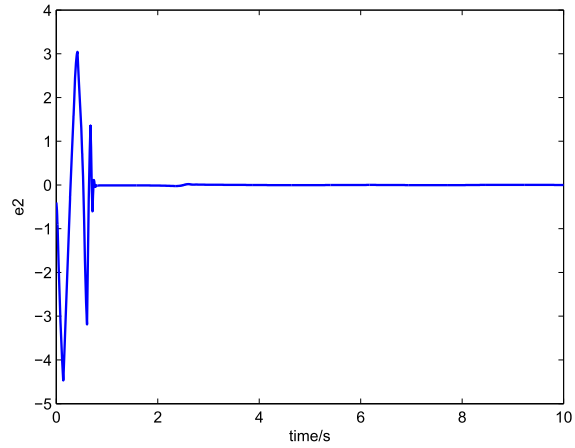

Fig. 7 Error dynamics of the states x_2 and y_2

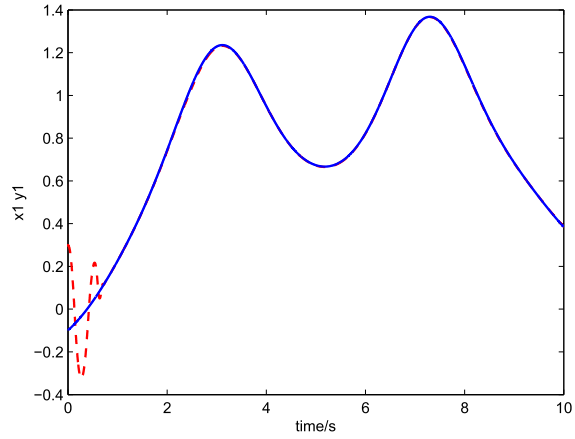

Fig. 8 Synchronization behaviors of the states x_1 and y_1

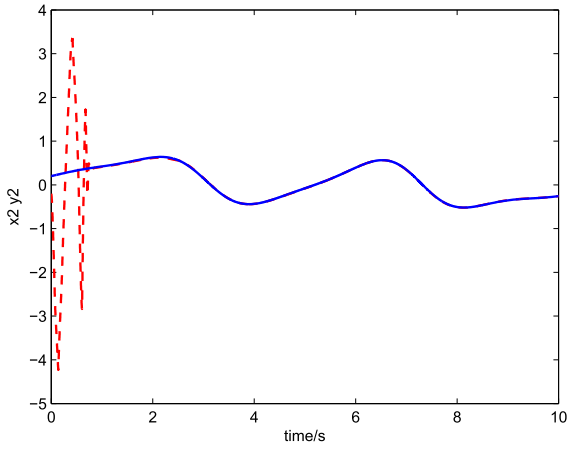

Fig. 9 Synchronization behaviors of the states x_2 and y_2

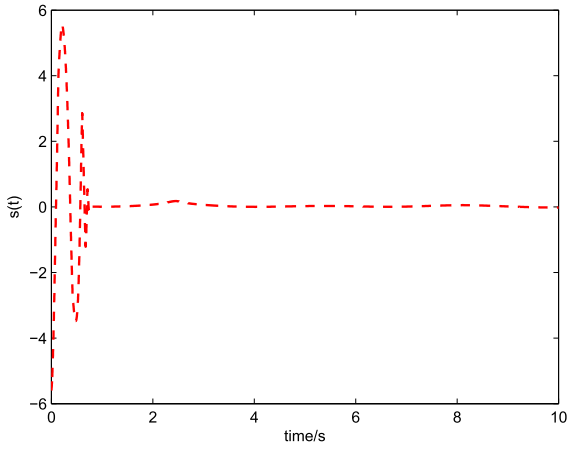

Fig. 10 Dynamic behavior of sliding surface

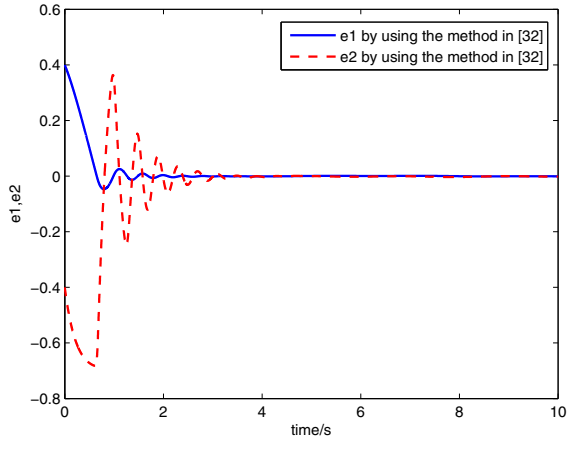

Fig. 11 Errors dynamics of Duffing–Holmes master system and Gyros slave system with the method in [32]

Choose the parameters as

$$a_{21} = 0.6, \quad b_{21} = -0.5, \quad c_1 = 35, \quad a_{22} = 0.68,$$
$$b_{22} = -0.54, \quad c_2 = 20, \quad r_f = r_g = r_\eta = 50.$$

Under these parameters, the maximum Lyapunov exponent of system (38) is computed as 0.0601, which shows this system is chaotic and surely unstable. In addition, the external disturbance is set as $d(t) = 0.05\sin(2t)$ and the initial conditions of the master and slave systems are chosen as $x(0) = [-0.81, -1.02, -0.5]^{\mathrm{T}}$ and $y(0) = [0.8, 1.2, 0.5]^{\mathrm{T}}$, respectively. The membership functions for x_i and y_i, $(i = 1, 2, 3)$ are selected as the following Gaussian functions:

$$\begin{aligned}
\mu A_1^i(x_i) &= \exp[-(x_i + 3)^2],\\
\mu A_2^i(x_i) &= \exp[-(x_i + 1)^2],\\
\mu A_3^i(x_i) &= \exp[-(x_i)^2],\\
\mu A_4^i(x_i) &= \exp[-(x_i - 1)^2],\\
\mu A_5^i(x_i) &= \exp[-(x_i - 3)^2].
\end{aligned} \tag{40}$$

The control effort of the slave system can be obtained as

$$u(t) = -c_1 e_2 - c_2 e_3 - \hat{f}(y, t) + \hat{g}(x, t) + \hat{\eta}\mathrm{sign}(s). \tag{41}$$

For free of control input, the phase portrait of the master and slave systems is given in Fig. 12 and the 2-D phase trajectories of different variables are shown in Figs. 13, 14 and 15, respectively. Under the proposed control effort, the 3-D phase portrait of synchronization of the master and slave systems is shown in Fig. 16, and the 2-D phase portrait of synchronization of the master and slave systems is shown in Figs. 17, 18 and 19, respectively. Figures 20, 21 and 22 show the error dynamics. Figures 23, 24 and 25 show the synchronization behaviors of state variables of the master and slave systems. It is noticeable that tracking errors converge to zero asymptotically, which verifies the effectiveness of our proposed control design method.

6 Conclusion

In this paper, an FO adaptive sliding mode control is proposed for chaos synchronization between two different uncertain FO chaotic systems with disturbance based on FO Lyapunov approach. A adaptive sliding mode control technique is established for chaos

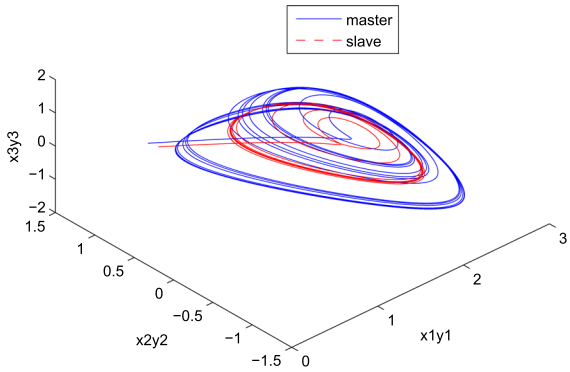

Fig. 12 3-D phase portrait of the Jerk chaotic master and slave systems without control

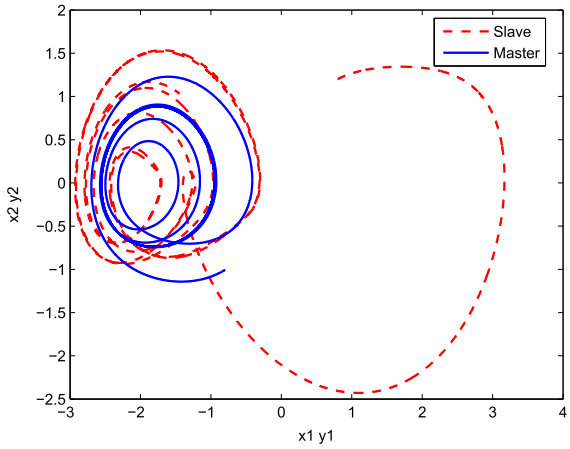

Fig. 13 2-D projection of the master and slave systems on (x_1, x_2)-plane and (y_1, y_2)-plane without control

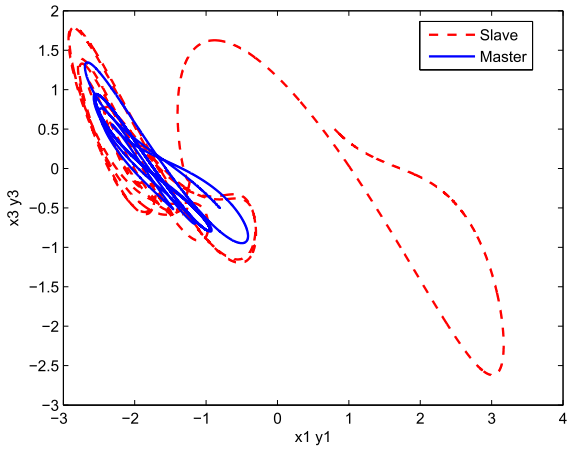

Fig. 14 2-D projection of the master and slave systems on (x_1, x_3)-plane and (y_1, y_3)-plane without control

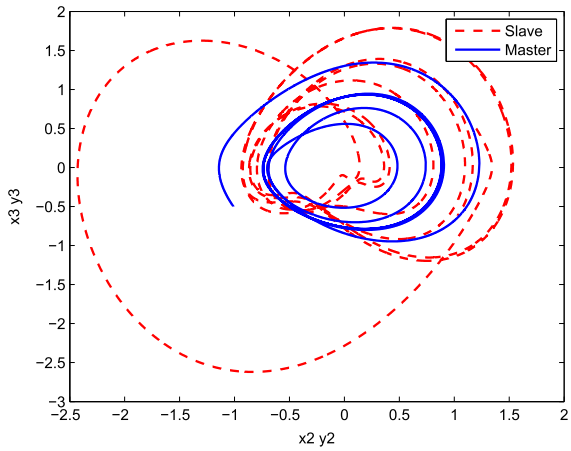

Fig. 15 2-D projection of the master and slave systems on (x_2, x_3)-plane and (y_2, y_3)-plane without control

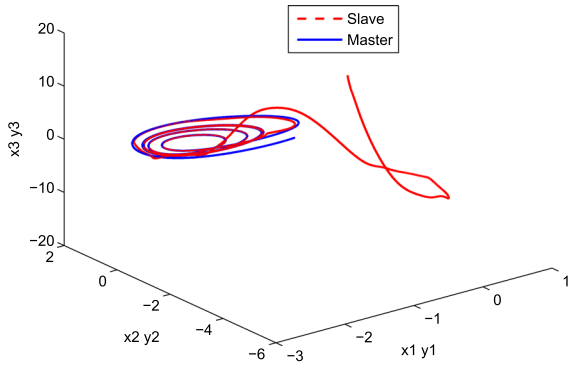

Fig. 16 3-D phase portrait of the jerk chaotic master and slave systems with control

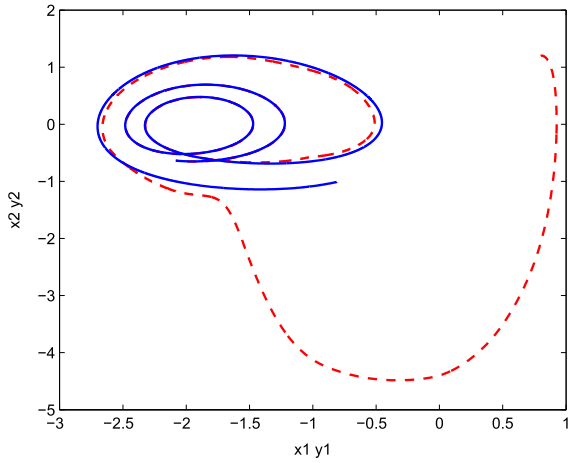

Fig. 17 2-D projection of the master and slave systems on (x_1, x_2)-plane and (y_1, y_2)-plane with control effort

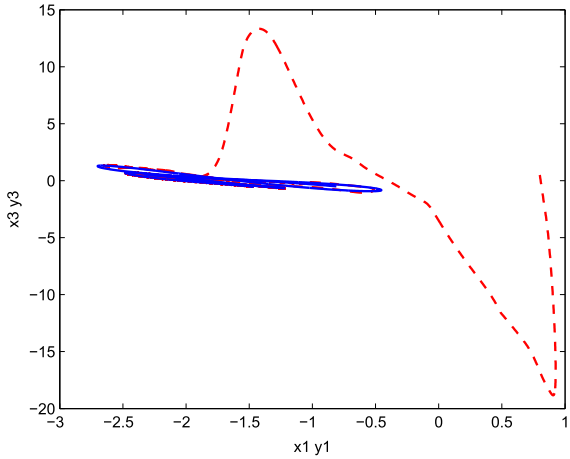

Fig. 18 2-D projection of the master and slave systems on (x_1, x_3)-plane and (y_1, y_3)-plane with control effort

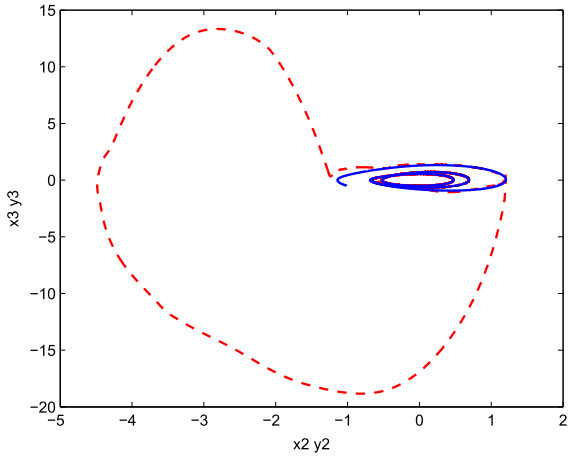

Fig. 19 2-D projection of the master and slave systems on (x_2, x_3)-plane and (y_2, y_3)-plane with control effort

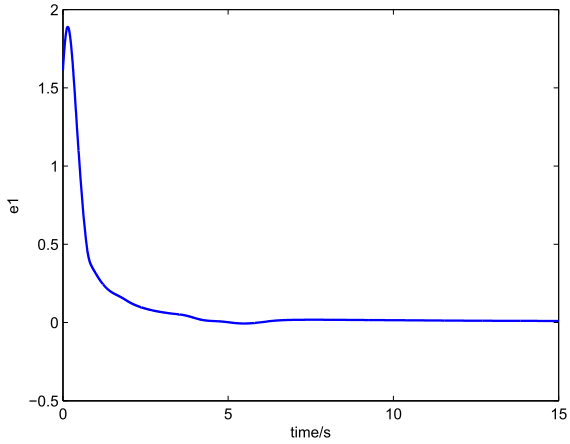

Fig. 20 Error dynamic of the states x_1 and y_1

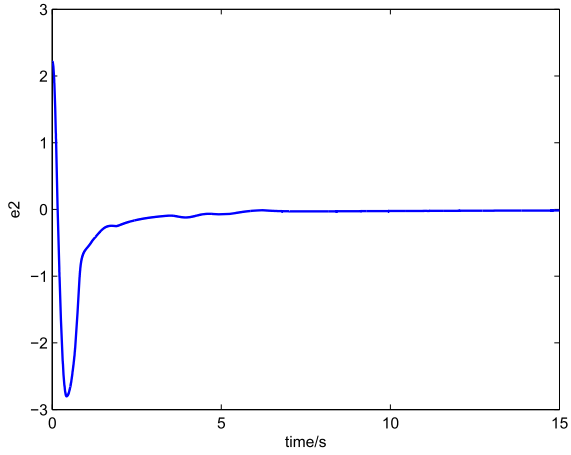

Fig. 21 Error dynamic of the states x_2 and y_2

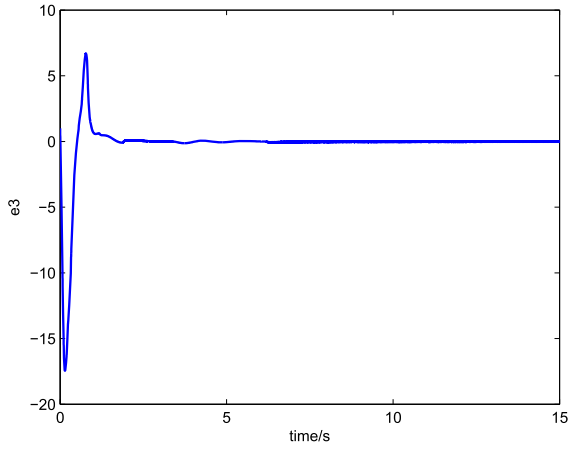

Fig. 22 Error dynamic of the states x_3 and y_3

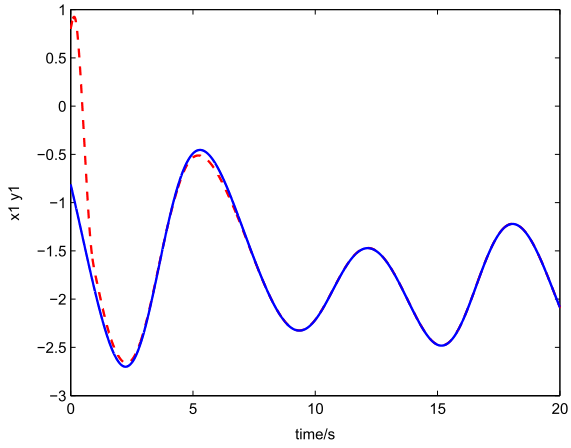

Fig. 23 Synchronization behavior of the state variables x_1 and y_1

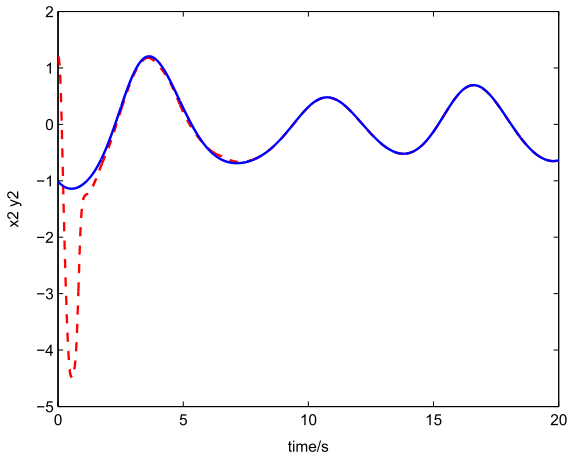

Fig. 24 Synchronization behavior of the state variables x_2 and y_2

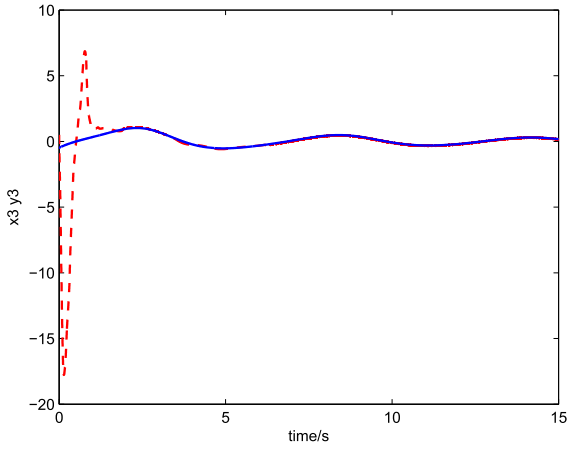

Fig. 25 Synchronization behavior of the state variables x_3 and y_3

synchronization of FO chaotic systems with external disturbances. A T–S fuzzy neural network model is introduced to approximate the uncertain terms and unknown upper bounds of some parameters. Furthermore, the corresponding adaptive laws are designed to tune online a set of free parameters. Two simulation examples, one of which consists of two nonidentical FO uncertain chaotic system, are given to demonstrate the effectiveness of the proposed method. Simulation results show that an asymptotical synchronization of the master and the slave systems can be achieved. On the other hand, how to eliminate the chattering caused by sign function in another way as well as to design a different sliding mode surface so that the systems have better synchronization effect is one of our primary works in the future.

Acknowledgements This work was supported in part by National Natural Science Foundation of China (Nos. 61603212, 51707102) and Hubei Provincial Department of Education for financial assistance through the "Chutian Scholar" program.

Compliance with ethical standards

Conflict of interest The authors declare that they have no conflict of interest.

References

1. Hilfer, R.: Applications of Fractional Calculus in Physics. World Scientific, River Edge (2001)
2. Arqub, O.A.: Numerical solutions for the Robin time-fractional partial differential equations of heat and fluid flows based on the reproducing kernel algorithm. Int. J. Numer. Methods Heat Fluid Flow **28**(4), 828–856 (2018)
3. Luo, Y., Chao, H., Di, L., Chen, Y.Q.: Lateral directional fractional order $(PI)^{\alpha}$ control of a small fixed-wing unmanned aerial vehicles: controller designs and flight tests. IET Control Theory Appl. **5**(18), 2156–2167 (2011)
4. Liu, H., Li, S., Wang, H., et al.: Adaptive fuzzy control for a class of unknown fractional-order neural networks subject to input nonlinearities and dead-zones. Inf. Sci. **454–455**, 30–45 (2018)
5. Sun, G., Ma, Z., Yu, J.: Discrete-time fractional order terminal sliding mode tracking control for linear motor. IEEE Trans. Ind. Electron. **65**(4), 3386–3394 (2018)
6. Song, S., Zhang, B., Song, X., et al.: Fractional order adaptive neuro-fuzzy sliding mode $H_{\inf}$ control for fuzzy singularly perturbed systems. J. Frankl. Inst. **356**(10), 5027–5048 (2019)
7. Song, S., Zhang, B., Song, X., et al.: Adaptive neuro-fuzzy backstepping dynamic surface control for uncertain fractional order nonlinear systems. Neurocomputing **360**, 172–184 (2019)
8. Haibo, B., Jinde, C., Jurgen, K.: State estimation of fractional-order delayed memristive neural networks. Nonlinear Dyn. **94**(2), 1215–1225 (2018)
9. Tejado, I., Milanes, V., Villagra, J., Vinagre, B.M.: Fractional network-based control for vehicle speed adaptation via vehicle-to-infrastructure communications. IEEE Trans. Control Syst. Technol. **21**(3), 780–790 (2013)
10. Sheng, D., Wei, Y., Cheng, S., Shuai, J.: Observer-based adaptive backstepping control for fractional order systems with input saturation. ISA Trans. **82**, 18–29 (2018)
11. Wei, Y., Sheng, D., Chen, Y., Wang, Y.: Fractional-order chattering-free robust adaptive backstepping control technique. Nonlinear Dyn. **95**, 2383–2394 (2019)
12. Yu, Y., Li, H.X., Wang, S., Yu, J.: Dynamical analysis of a fractional order Lorenz chaotic system. Chaos Solitons Fractals **42**, 1181–1189 (2009)
13. Tavazoei, M.S., Haeri, M.: Chaotic attractors in incommensurate fractional order chaotic system. Phsica D **237**, 2628–2637 (2008)

14. Hajipour, A., Aminabadi, S.S.: Synchronization of chaotic Arneodo system of incommensurate fractional order with unknown parameters using adaptive method. Optik **127**(19), 7704–7709 (2016)
15. Jajarmi, A., Hajipour, M., Baleanu, D.: New aspects of the adaptive synchronization and hyperchaos suppression of a financial model. Chaos Solitons Fractals **99**, 285–296 (2017)
16. Mohadeszadeh, M., Delavari, H.: Synchronization of uncertain fractional-order hyperchaotic systems via a novel adaptive interval type-2 fuzzy active sliding mode controller. Int. J. Dyn. Control **5**(1), 135–144 (2017)
17. Lin, T.-C., Lee, T.-Y., Balas, V.E.: Adaptive fuzzy sliding mode control for synchronization of uncertain fractional order chaotic systems. Chaos Solitons Fractals **44**(10), 791–801 (2011)
18. Jafari, P., Teshnehlab, M., Tavakoli-Kakhki, M.: Synchronization and stabilization of fractional order nonlinear systems with adaptive fuzzy controller and compensation signal. Nonlinear Dyn. **90**(2), 1037–1052 (2017)
19. Khan, A., Tyagi, A.: Fractional order disturbance observer based adaptive sliding mode synchronization of commensurate fractional order Genesio–Tesi system. AEU Int. J. Electron. Commun. **82**, 346–357 (2017)
20. Megherbi, O., Hamiche, H., Djennoune, S., et al.: A new contribution for the impulsive synchronization of fractional-order discrete-time chaotic systems. Nonlinear Dyn. **90**(3), 1519–1533 (2017)
21. Mohammadzadeh, A., Ghaemi, S.: Robust synchronization of uncertain fractional-order chaotic systems with time-varying delay. Nonlinear Dyn. **93**(4), 1809–1821 (2018)
22. Tabasi, M., Balochian, S.: Synchronization of the chaotic fractional-order Genesio–Tesi systems using the adaptive sliding mode fractional-order controller. J. Control Autom. Electr. Syst. **29**(1), 15–21 (2018)
23. Boubellouta, A., Zouari, F., Boulkroune, A.: Intelligent fuzzy controller for chaos synchronization of uncertain fractional-order chaotic systems with input nonlinearities. Int. J. Gen. Syst. **48**(3), 1–24 (2019)
24. Bao, H., Park, J.H., Cao, J.: Adaptive synchronization of fractional-order memristor-based neural networks with time delay. Nonlinear Dyn. **82**(3), 1343–1354 (2015)
25. Haibo, B., Park, J.H., Cao, J.: Synchronization of fractional-order complex-valued neural networks with time delay. Neural Netw. **81**, 16–28 (2016)
26. Lin, D., Wang, X., Yao, Y.: Fuzzy neural adaptive tracking control of unknown chaotic systems with input saturation. Nonlinear Dyn. **67**(4), 2889–2897 (2012)
27. Diethelm, K., Ford, N.J., Freed, A.D.: Detailed error analysis for a fractional Adams method. Numer. Algorithms **36**(1), 31–52 (2004)
28. Aguila Camacho, N., Duarte Mermoud, M.A., Gallegos, J.A.: Lyapunov functions for fractional order systems. Commun. Nonlinear Sci. Numer. Simul. **19**(9), 2951–2957 (2014)
29. Lenka, B.K., Banerjee, S.: Sufficient conditions for asymptotic stability and stabilization of autonomous fractional order systems. Commun. Nonlinear Sci. Numer. Simul. **56**, 365–379 (2018)
30. Chen, D., Zhang, R., Liu, X., Ma, X.: Fractional order Lyapunov stability theorem and its applications in synchronization of complex dynamical networks. Commun. Nonlinear Sci. Numer. Simul. **19**(12), 4105–4121 (2014)
31. Castro, J.L.: Fuzzy lofic controllers are universal approximators. IEEE Trans. Syst. Man Cybern. **25**(4), 629–635 (1995)
32. Delavari, H.: A novel fractional adaptive active sliding mode controller for synchronization of non-identical chaotic systems with disturbance and uncertainty. Int. J. Dyn. Control **5**, 102–114 (2017)